Anisotropic prestack depth migration processing in the Permian Basin, Texas

Ananya Roy, Lin Zheng, Xin Hu, CGG*
Robin Pearson, Ernesto V. Oropeza, Sarah Mueller, Mark Chang, Anadarko Petroleum Corporation

Summary

The Wolfcamp reservoir of the Permian Basin has recently generated interest for its potentially vast oil and gas reserves. Imaging this reservoir using seismic data is challenging despite the uncomplicated geology at reservoir depth, because of the complexity of the near-surface in this region. In this work, we apply a modern anisotropic prestack depth migration (APSDM) processing flow to Permian Basin data and find that it improves the resolution of near-surface anomalies and imaging at the reservoir compared to the legacy prestack time migration.

Introduction

The Permian Basin lies in West Texas and South Eastern New Mexico and it comprises the Delaware and Midland Basins separated by the uplifted Central Basin Platform (Figure 1). Oil and gas reserves were first discovered here in 1921 and since then production has been steadily driven by new discoveries and advances in extraction techniques such as horizontal drilling and hydraulic fracturing (Texas RRC, 2016).

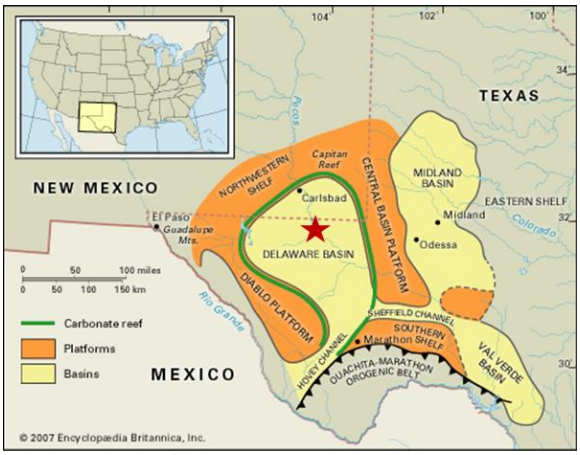

Figure 1: A map of the Permian Basin in West Texas and South Eastern New Mexico (Encyclopedia Britannica, 2013). The star marks the location of the Tunstill survey.

Figure 2 shows a time migration image from the Delaware Basin area. The Wolfcamp reservoir, which has recently generated interest for its potential (Gaswirth et al., 2016), lies about 12,000 ft below the surface and is on average 3000 ft thick in this region. The geology at reservoir depth seems fairly simple with little large-scale lateral variations. The near-surface, however, is quite complex. It includes a layer of salt, roughly 300 ft thick, with a top of salt (TOS) that is rugose and poorly imaged. In addition, as in other parts of the Permian basin, the salt body contains karst features which are formed by the dissolution of shallow evaporites by groundwater flow. Correctly understanding this high velocity and laterally complex near-surface is challenging. We applied an anisotropic prestack depth migration (APSDM) processing flow with model building in depth to this Delaware Basin data. To improve on the legacy (2007) prestack time migration (PSTM) effort, full waveform inversion (FWI) was used to estimate the overburden velocities more accurately, velocities were tied to well markers, and processes such as 5D interpolation and rank reduction denoise were applied to improve the S/N.

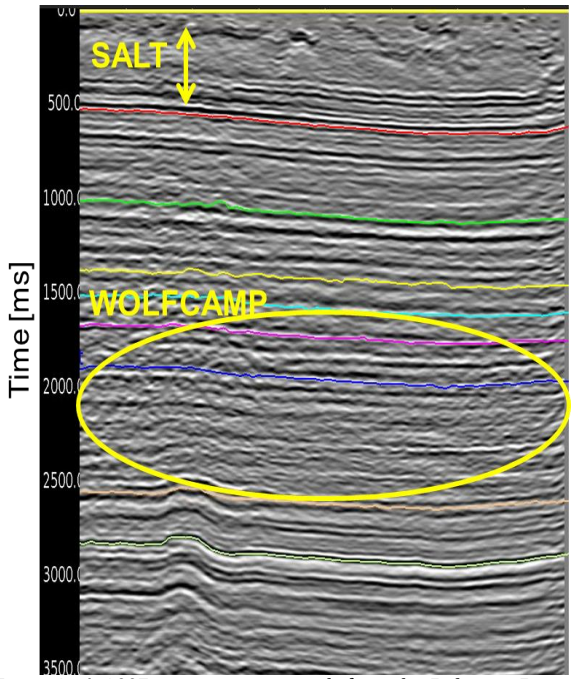

Figure 2: A 2007 time migration stack from the Delaware Basin region marked by the star in Figure 1.

APSDM in the Permian Basin

The data presented here are from a 75 sq. mile area of the Tunstill survey located in the northern section of the Delaware Basin (marked by the star in Figure 1). The survey was acquired in 2006 using Vibroseis. The acquired data have high levels of noise originating from ground roll, guided waves, and scattering from shallow evaporites. A selection of data from the most challenging part of the

survey is shown in Figure 3, where target events are completely masked by noise on the raw CDP gathers.

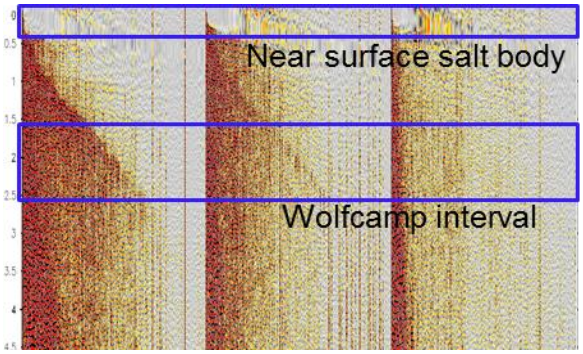

Figure 3: Raw CDP gathers with normal moveout applied show the high level of noise contamination in the data.

Impact of depth model building and FWI

Since the near-surface does not have enough useable offsets for curvature-based reflection tomography (Figure 3), refraction tomography (Zhu et al., 2000) is typically used to estimate the near-surface velocity. In this work, refraction FWI (Mei et al., 2014) was used as part of a depth velocity building flow to improve the resolution of velocity anomalies in the complex near-surface salt body. FWI was challenging because the 6 Hz low frequency cut-off on the acquisition sweep made the S/N below 6 Hz poor. To avoid cycle skipping with FWI in the absence of low frequencies, an initial model was built using iterative refraction tomography and was followed by refraction FWI from 7 Hz to 10 Hz.

Despite the challenges, the FWI-derived near-surface model resolved the rugose TOS well enough to generate a base of salt (BOS) image with very little distortion (Figure 4). The BOS is nearly flat, just as the well markers (shown in red) suggest it should be. Since no diving rays penetrate the large velocity contrast at the BOS, refraction FWI was not useful below the salt body. The model below the salt was built using reflection tomography and well log information. A depth migration with this model tied the well markers (Figure 4) without the need for any post-migration processing, like a 1D stretch, to tie the wells. Anisotropy parameters, δ and ε, were chosen to flatten migration gathers with this velocity model. The value of δ increases gradually from ~1% in the shallow salt to ~9% in the Wolfcamp interval. The ratio between ε and δ is ~2.

Compared to the legacy PSTM flow, which compensated the near-surface with 1D static shifts computed from refraction tomography, APSDM using the FWI near-surface model imaged the near-surface TOS better (Figure 5). FWI also improved the imaging of karsts in the salt body. These collapse-features are not always visible above the surface, and their detection using seismic data can help prevent drilling incidents. On a depth slice through the salt body, karst features look like isolated anomalies and can be spotted on both the time and depth migration volumes (Figure 6); however, those on the APSDM stack are clearer and more reliable (Figure 7). On the legacy PSTM images, the BOS below the karst features is locally pulled-up, indicating that the karst velocity anomalies are not correctly resolved and the reflectors under the anomalies are less reliable than on the depth migration image.

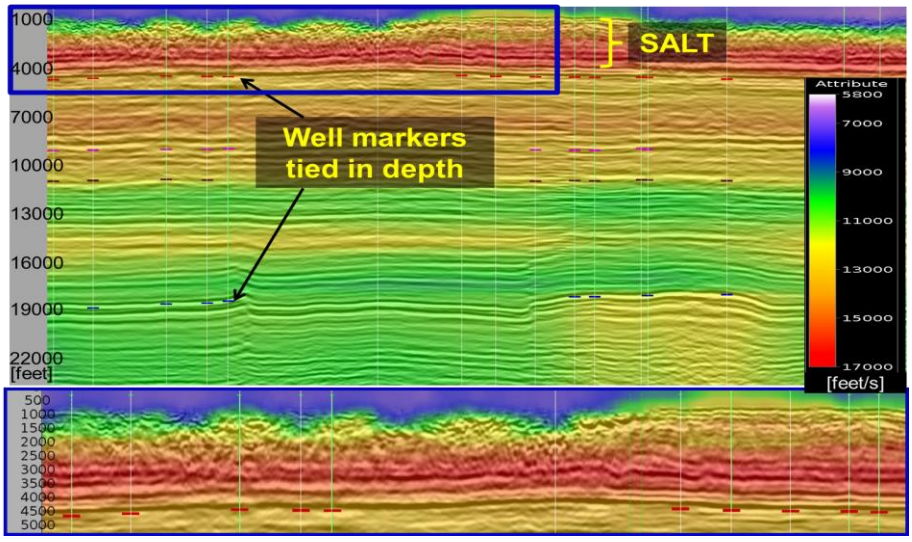

Figure 4: Depth velocity model overlaid on the 2016 APSDM stack. A zoomed-in panel shows the near-surface model from FWI, with BOS well markers annotated as red dashes.

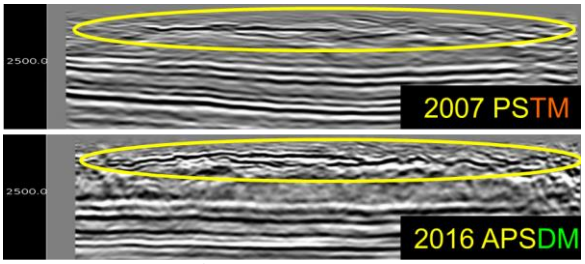

Figure 5: TOS images for the PSTM and APSDM stacks. APSDM, with an FWI-derived near-surface model, images the TOS better.

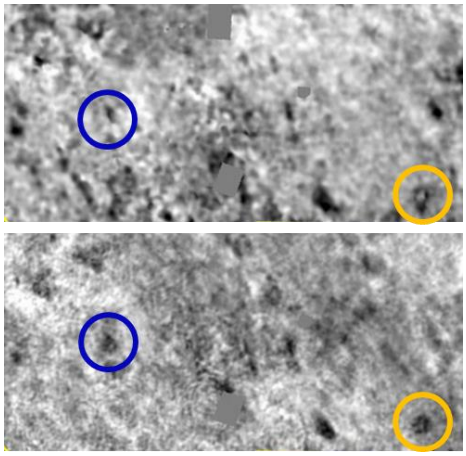

Figure 6: Depth slices through the shallow salt body, 850 m above the BOS, show karst features on the 2007 PSTM stack stretched to depth (top) and 2016 APSDM stack (bottom). The karsts circled in blue and orange are compared in Figure 7.

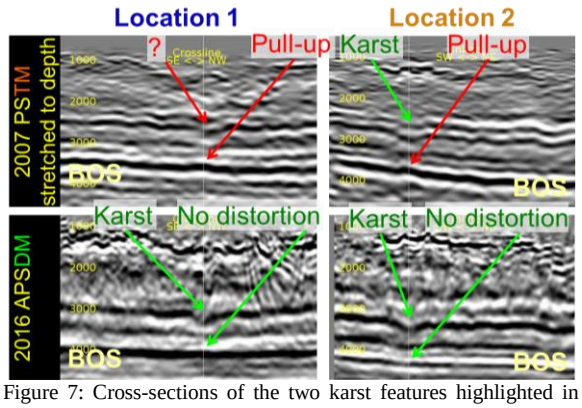

Figure 7: Cross-sections of the two karst features highlighted in Figure 6 show these anomalies are better resolved on the APSDM.

Impact of advanced denoise and 5D interpolation

The 2007 legacy time processing flow included ground roll attenuation, several iterations of de-spike, and Radon de-multiple for noise attenuation. In the 2016 depth processing flow, S/N was further improved by the addition of rank reduction denoise (Sternfels et al., 2015) and 5D interpolation (Trad, 2007), as shown in Figure 8. The improved noise attenuation coupled with the quadrupled fold from 5D interpolation generated a superior image at the Wolfcamp reservoir compared to the legacy time migration (Figure 9). The PSDM image has better S/N, and this can help interpretation near faults as demonstrated in Figure 10. On the legacy time migration image, it is unclear how far the fault extends. The fault and its vertical extent are much clearer on the PSDM image.

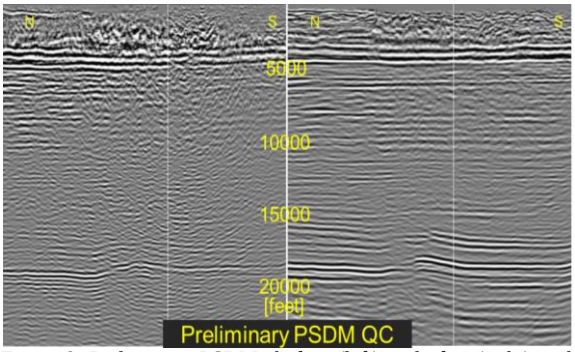

Figure 8: Preliminary PSDMs before (left) and after (right) rank reduction denoise and 5D interpolation show their impact on S/N

Discussion

After the APSDM processing flow, CDP gathers that were previously dominated by noise show reflectors at reservoir depth, but they also reveal an azimuthal jitter (Figure 11). While this azimuthal variation could be evidence of reservoir fractures, it could also be the result of residual errors in the overburden velocity. Even though FWI has significantly improved the near-surface model, its accuracy is limited by the coarse acquisition geometry of this survey. An image of the near-surface, perpendicular to the receiver lines (Figure 12), shows that the TOS is not imaged in the space between the receiver lines. The coarse receiver line spacing of 1540 ft limits our ability to clearly define the position of the large velocity contrast at the TOS. This limits the accuracy of our near-surface model and, in turn, the accuracy of all the underlying reflectors. An accurate near-surface velocity is important for decoupling the imprint of shallow velocity errors from the properties of the reservoir. We have shown that the accuracy of the near-surface model improves with FWI, but we also need an acquisition geometry that is dense enough to sample the complexities of the near-surface, at least twice the current density, before we can make a meaningful analysis of more subtle properties such as azimuthal velocity variation. Such azimuthal analysis will also require a larger maximum crossline offset, approximately twice the existing value of 10,780 ft, for sufficient angle coverage at target depth. Finally, a low-noise broadband source (Castor et al., 2015)

will improve the S/N at low-frequencies which could further improve the ability of FWI to estimate the near surface velocity.

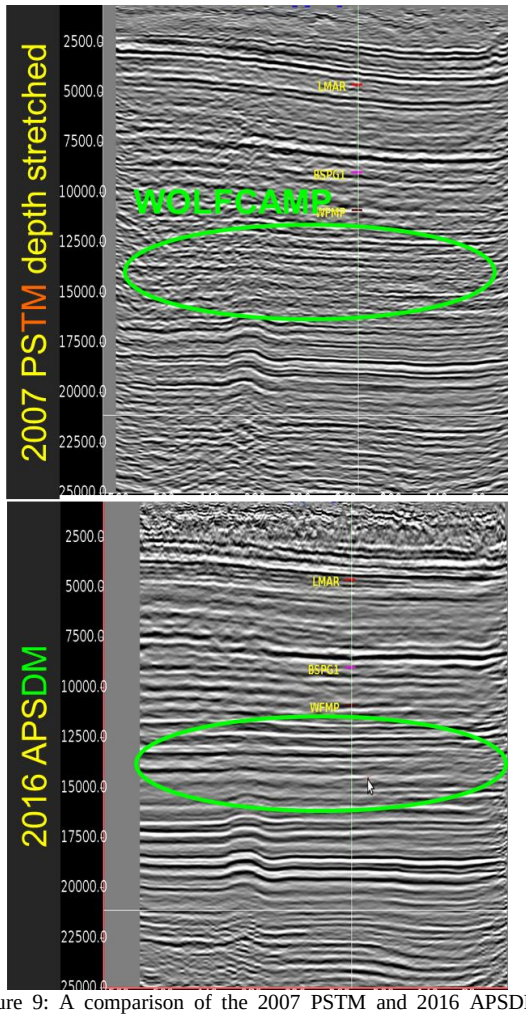

Figure 9: A comparison of the 2007 PSTM and 2016 APSDM stacks. The APSDM includes advanced denoise processing and 5D interpolation in addition to migration with a depth velocity model.

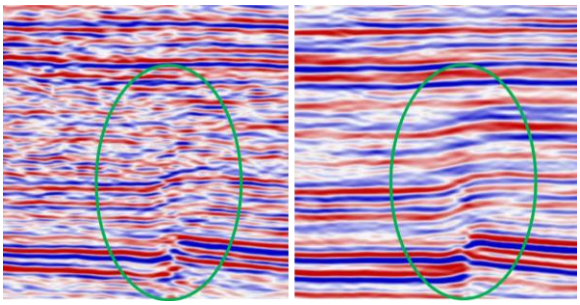

Figure 10: Legacy PSTM (left) and APSDM (right) migration images near a fault just below the reservoir interval.

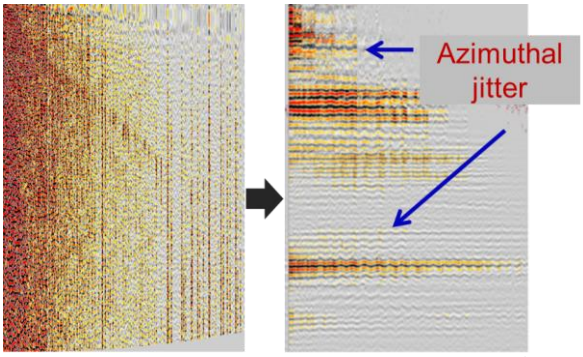

Figure 11: Raw gathers (shown with NMO on the left) are dominated by noise. After depth processing, the common-offset-common-angle (COCA) migration gather (right) shows clear events at reservoir depth and an azimuthal jitter.

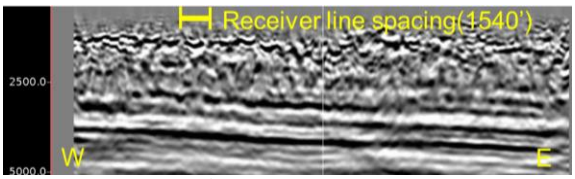

Figure 12: A near surface image, perpendicular to the receiver lines, shows scalloping at the TOS due to coarse line spacing.

Conclusion

An APSDM workflow improved seismic imaging in the Delaware Basin region of the Permian Basin, where the regional geology of the Wolfcamp reservoir is simple, but the near-surface is complex. The comparisons in this paper show that modern denoise, interpolation, and depth model building, including refraction and reflection tomographic inversion and FWI, can improve resolution of the overburden velocity and imaging at the reservoir while also generating a realistic velocity model that ties well markers in depth. If PSDM processing is also supported by an acquisition geometry that is dense enough to sample the lateral changes in the near-surface, its imprint on the underlying reflectors could be further reduced. This should be the first step towards drawing better conclusions about reservoir-scale seismic attributes in this region.

Acknowledgments

We would like to thank our colleagues, Erasmo Rodriguez, Tunde Markos, Jiawei Mei, Jeshurun Hembd, Yan Huang, and Sue Rezai at CGG for help with processing and for valuable discussions. We would also like to thank our colleagues at Anadarko, Stella Braz and Alan Gunnell, for their feedback on processing and Tim Fasnacht for valuable suggestions on this paper. We are grateful to the CGG Multi Client Data Library for providing us use of the data and the Legacy PSTM volume.

EDITED REFERENCES

Note: This reference list is a copyedited version of the reference list submitted by the author. Reference lists for the 2017 SEG Technical Program Expanded Abstracts have been copyedited so that references provided with the online metadata for each paper will achieve a high degree of linking to cited sources that appear on the Web.

REFERENCES

Castor, K., T. Bianchi, O. Winter, and T. Klein, 2015, Efficient harmonic-distortion mitigation on vibro-seismic sources: Presented at the EAGE Workshop on Broadband Seismic, Extended Abstracts, BS08.

Encyclopedia Britannica, 2013, Permian Basin, https://www.britannica.com/place/Permian-Basin, accessed 1 March 2017.

Gaswirth, S. B., K. R. Marra, P. G. Lillis, T. J. Mercier, H. M. Leathers-Miller, C. J. Schenk, T. R. Klett, P. A. Le, M. E. Tennyson, S. J. Hawkins, M. E. Brownfield, J. K. Pitman, and T. M. Finn, 2016, Assessment of undiscovered continuous oil resources in the Wolfcamp shale of the Midland Basin, Permian Basin Province, Texas, 2016: U.S. Geological Survey Fact Sheet 2016-3092.

Mei, J., S. Ahmed, A. Searle, and C. Ting, 2014, Application of full waveform inversion on Alaska land 3D survey: 84th Annual International Meeting, SEG, Expanded Abstracts, 981–986, http://dx.doi.org/10.1190/segam2014-0505.1.

Sternfels, R., G. Viguier, R. Gondoin, and D. Le Meur, 2015, Joint low-rank and sparse inversion for multidimensional simultaneous random/erratic noise attenuation and interpolation: 77th Annual International Conference and Exhibition, EAGE, Extended Abstracts, We N112 04.

Texas RRC., 201, Permian Basin Information, http://www.rrc.state.tx.us/oil-gas/major-oil-gas-formations/permian-basin/, accessed 1 March 2017.

Trad, D., 2007, A strategy for wide-azimuth land interpolation: 77th Annual International Meeting, SEG, Expanded Abstracts, 946–950, http://dx.doi.org/10.1190/1.2792562.

Zhu, T., S. Cheadle, A. Petrella, and S. Gray, 2000, First-arrival tomography: Method and application: 70th Annual International Meeting, SEG, Expanded Abstracts, 2028–2031, http://dx.doi.org/10.1190/1.1815839.